ELSEVIER

Polymer 42 (2001) 9627–9631

polymer

www.elsevier.com/locate/polymer

Epitaxial act of sodium 2,2′-methylene-bis-(4,6-di-*t*-butylphenylene) phosphate on isotactic polypropylene

Shiho Yoshimoto[a], Takahiko Ueda[a], Keiji Yamanaka[a], Akiyoshi Kawaguchi[a,*], Etsuo Tobita[b], Tohru Haruna[b]

[a]*Faculty of Science and Engineering, Ritsumeikann University, Noji-Higashi 1-1-1, Kasatsu, Shiga 525-8577, Japan*
[b]*Asahi Denka Kogyo K.K., 5-2-13 Shirahata, Urawa City, Saitama 336-0022, Japan*

Received 9 March 2001; accepted 8 June 2001

Abstract

Sodium 2,2′-methylene-bis-(4,6-di-*t*-butylphenylene)phosphate(NA-11) is widely used as a nucleating agent in the processing of isotactic polypropylene(iPP). To reveal its act as the nucleating agent on iPP, the crystallization behavior of NA-11 on isotactic polypropylene was investigated. NA-11 was crystallized on the oriented, thin iPP film from the solution in dimethyformamide at various temperatures. iPP was also crystallized from the melt on NA-11 crystals grown from ethanol. The samples thus prepared were examined by electron microscopy. NA-11 epitaxially crystallized on the iPP substrate at high temperatures, performing the crystallographical relationship, $[010]_{NA\text{-}11}//[001]_{iPP}$ and $(001)_{NA\text{-}11}//(010)_{iPP}$, and iPP on the NA-11 crystals with the same orientational relationship.

Keywords: Isotactic polypropylene; ADK STAB NA-11; Electron diffraction

1. Introduction

Isotactic polypropylene (iPP) is one of the world-widely used convenient plastics and its demand is expected to increase. Thus, from the commercial point of view, it is a very important issue to enhance the physical properties of iPP such as mechanical strength, thermal stability, optical opaqueness etc. It is known that nucleating agents added in the processing play an important role for the purpose. Sodium 2,2′-methylene-bis-(4,6-di-*t*-butylphenylene)phosphate (commercial name of ADK STAB NA-11 (abbreviated to NA-11 here), developed by Asahi Denka Kogyo [1]) is one of the most useful nucleating agents and widely used. So far, it is said that the effectiveness of a nucleating agent depends on the epitaxial crystallization between itself and the processed plastics, e.g. in the present case iPP. In the present works, following experiments were undertaken for examining the effect of NA-11 as a nucleating agent: (1) iPP was crystallized on NA-11 crystals from the melt, and (2) NA-11 was crystallized on the highly drawn, thin iPP film from the dilute solution in various solvents by changing the crystallization temperature. The samples thus prepared were examined by transmission electron microscopy. It is made clear that NA-11 crystallites are over-grown on the iPP film, performing the epitaxial relationship to iPP, and vice versa.

2. Experimental

Following two experiments were carried out.

1. NA-11 was crystallized on a glass plate from the solution in ethanol by the solvent evaporation method at various temperatures. A thin, oriented iPP film, which was prepared by the method developed by Petermann and Gohil [2], was put on the thus-crystallized NA-11. The glass plate was heated up to a temperature higher than the melting temperature of iPP, and after kept at the temperature for a while, e.g. for 10 min, it was cooled down to the ambient temperature so that iPP was induced to crystallize onto NA-11 crystals.
2. Firstly, a uniaxially oriented, thin iPP film was prepared by the Petermann and Gohil method. The film was put on the glass plate and heated up to a given temperature, e.g. 140°C, and kept at the temperature. In parallel, the solution of NA-11 in dimethyformamide was heated up to the same temperature. Several drops of the solution were put on the iPP film, and by evaporation of solvent, NA-11 was crystallized on the iPP film at the temperature.

* Corresponding author. Fax: +81-77-561-2659.
E-mail address: akiyoshi@se.ritsumei.ac.jp (A. Kawaguchi).

0032-3861/01/$ - see front matter
PII: S0032-3861(01)00510-9

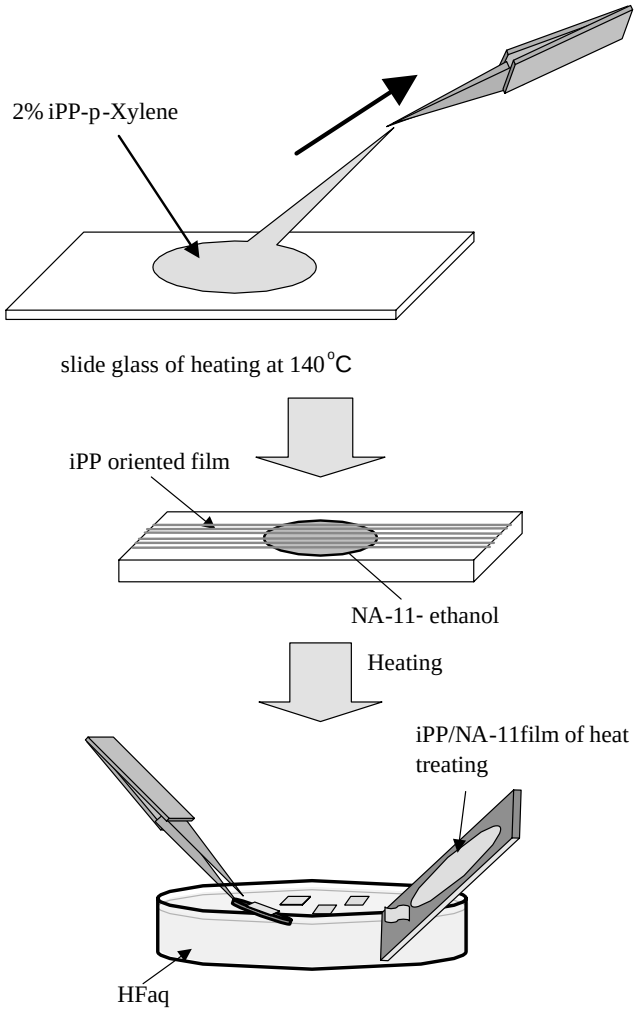

Fig. 1. Sketch of the procedure to prepare specimens for electron microscopy.

The procedure for preparing specimens for electron microscopy is shown schematically in Fig. 1. The specimens were examined by transmission electron microscopy. Further, thermal properties of NA-11 crystals were examined by DSC and TGA measurements. The heating rate for DSC and TGA measurements was 10°C/min.

3. Results and discussion

Fig. 2 shows the DSC and TGA thermograms of NA-11 crystals grown from the solution in ethanol. Curve I indicates the DSC curve for heating the as-prepared NA-11 sample which was well-dried by air-drying for about a week. After the original sample was heated up to 290°C, it was cooled down to room temperature, and subsequently, the sample was again heated up to 450°C. Curve II shows the DSC thermogram for the second heating.

The TGA curve of as-prepared sample corresponds to Curve I of DSC thermogram. Around the temperature

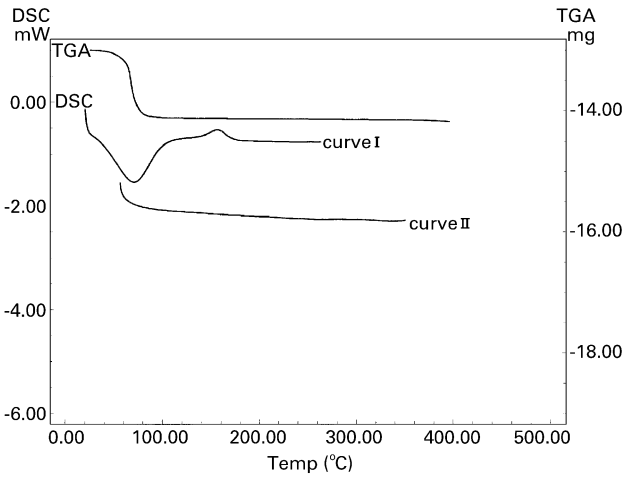

Fig. 2. DSC and TGA curves by heating. Curve I of DSC is for NA-11 crystals prepared from alcohol and dried, and Curve II is measured by the second heating of Curve I. In both DSC and TGA measurements, the heating rate is 10°C/min.

where the broad endothermic peak of Curve I starts, the sample weight is markedly reduced and thereafter leveled off. This explains that the endotherm is caused by removal of ethanol contained in the sample. The subsequent exotherm shows the crystallization or transformation of NA-11. The endothermic and exothermic peaks disappear in the second heating. It is considered that alcohol molecules could not be simply absorbed on NA-11 crystallites, but incorporated in NA-11 crystals as a crystalline moiety. Intact NA-11 crystals exhibit a complicated endotherms having multiple endothermic peaks in the same temperature range as the broad endotherm of Curve I and a sharp endothermic peak at 137.7°C. Thus, NA-11 crystals behave in various ways depending on the degree of content of ethanol. From the above results, it is understood that once the NA-11 samples are heated over 200°C, alcohol is removed completely and NA-11 crystallites take a stable crystalline form. NA-11 crystals actually experience, in the processing of iPP, a temperature where their crystalline state transform into a stable form after removal of ethanol even if they are produced from alcohol. Further, since the crystalline state of NA-11 containing alcohol is unknown at the present time, the crystalline state of as-prepared NA-11 crystals is not referred to here. On the other hand, NA-11 crystals grown from the DMF show no endothermic peak in DSC and have a stable crystalline form.

Highly drawn iPP was put on NA-11 crystals grown from alcohol and was annealed in the temperature range of 170–176°C. Fig. 3 shows an electron micrograph (EM) of one of thus prepared samples and the corresponding electron diffraction pattern (ED pattern). Rod-like NA-11 crystals were grown aligning their long side parallel. By annealing in the temperature range, the oriented iPP is largely shrunk macroscopically, and the molecular orientation is disordered. At rather low temperature in comparison with the melting temperature, iPP was not completely in the molten

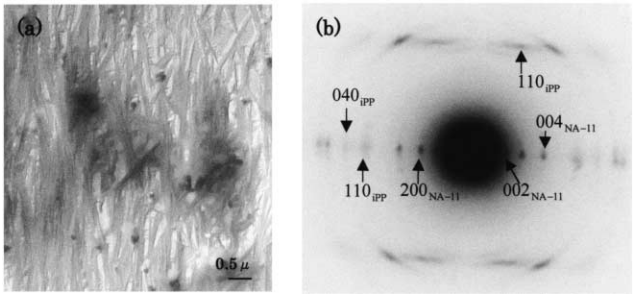

Fig. 3. (a) Electron micrograph of the specimen prepared as follows: NA-11 crystals were grown from alcohol, and drawn iPP was put on the crystals and heated in the temperature range of 170–176°C. Shadowed with Pt–Pd. (b) Corresponding electron diffraction pattern.

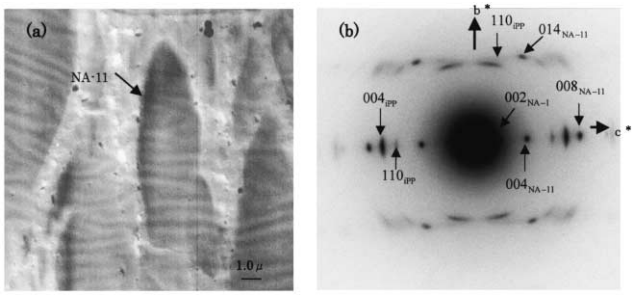

Fig. 5. (a) Electron micrograph of the specimen prepared as follows: NA-11 crystals were grown from alcohol at a rather high temperature, and drawn iPP was put on the crystals and heated at 190°C. Shadowed with Pt–Pd. (b) Corresponding electron diffraction pattern.

state, but experienced the 'partial melting'. To reveal the crystalline feature of iPP, NA-11 was dissolved out by washing with ethanol. Fig. 4 shows the EM and ED pattern of a sample after such treatment. In some cases, oval-shaped and rectangular crystals are grown. Figs. 5 and 6 show the cases of oval-shaped crystals. Fig. 5 shows the EM and ED of the oval-shaped crystals on which iPP was crystallized from the molten state, and Fig. 6 those of the sample from which NA-11 crystals were removed by alcohol.

The ED patterns in Figs. 3(b) and 5(b) are identical and schematized in Fig. 7 in the reciprocal lattice. Diffraction spots of iPP are indexed with the α-form [3] and those of NA-11 on the basis of the crystallographic data [4]. We see that both iPP and NA-11 crystals exhibit, basically, the net patterns like those of single crystals, and further that the definite relationship holds between two patterns. As seen in Fig. 3(b), the 110_{iPP} spots of iPP are on the first layer line, and the 040_{iPP} spots on the equator. It is found thus that the *a*-axis of iPP is parallel to the long axis of the rod-like crystals of NA-11 in Fig. 3 and of the oval-shaped crystals in Fig. 5. Figs. 4(b) and 6(b) show only the ED pattern of iPP as the NA-11 crystals are removed. These make clear the above-mentioned orientation of iPP, that is, the *a*-axis of iPP is meridional and the *b*-axis is horizontal. On the other hand, in the ED pattern of NA-11, the 002 and 004 spots are on the equator, and 014 spot nearly on the first layer line of iPP. Clearly, the crystallographic orientational relationship holds between iPP and NA-11. At the first sight, we notice the following crystallographic feature: the orientational relationship of the *a*-axis of iPP//the *b*-axis of NA-11 and the *b*-axis of iPP//the *c*-axis of NA-11 holds between iPP and NA-11. It is to be noted here, however, that the 110_{iPP} spots (indicated with arrows in Fig. 7) are observed on the equator in the ED patterns of Figs. 4–6. This is never explained in terms of the above first orientational relationship. This implies that the *c*-axis of iPP should be parallel to the meridional direction in these ED patterns. In other words, the *c*-axis is normal to the figures' plane in the first case of orientational relationship, and to the contrary the *a*-axis is normal to it in the second case. Strictly speaking, the 110_{iPP} diffraction of interest is never observed in this orientation of the *c*-axis while the *b*-axis is horizontal. In reality, iPP crystallites could change their orientation by twisting back and force around the *c*-axis and as a result, the 110_{iPP} diffraction becomes observable. Thus, it is possible that the second orientational relationship of the *c*-axis of iPP//the *b*-axis of NA-11 should be attained.

Fig. 8 shows an EM of the uniaxially oriented, thin iPP film on which NA-11 was crystallized by the way as described in (2) in Section 2. NA-11 crystals grow extending largely in the direction parallel to the molecular axis of iPP. As indexed, the 014 and other 01*l* spots of NA-11 are nearly on the first layer line of iPP and the 00*l* spots on the

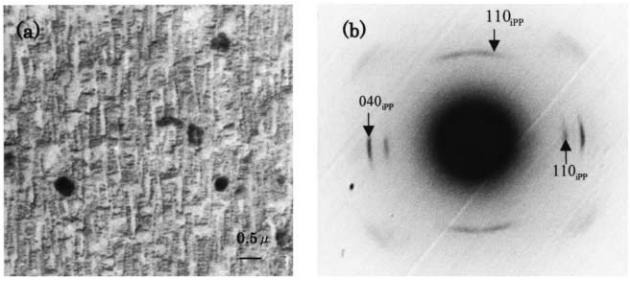

Fig. 4. (a) Electron micrograph of the sample prepared as follows: thin film was prepared in the same way as in the case of Fig. 3(a) and subsequently NA-11 crystals were washed out with alcohol. Shadowed with Pt–Pd. (b)Corresponding electron diffraction pattern.

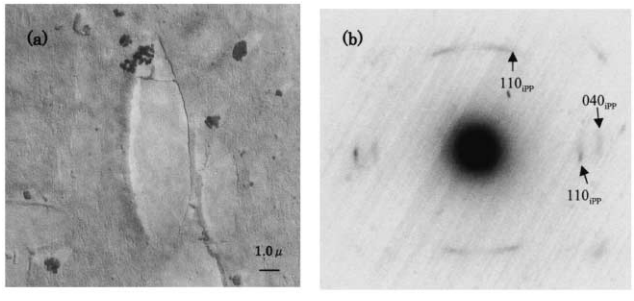

Fig. 6. (a) Electron micrograph of the sample prepared as follows: thin film was prepared in the same way as in the case of Fig. 5 and subsequently NA-11 crystals were washed out with alcohol. Shadowed with Pt–Pd. (b)Corresponding electron diffraction pattern.

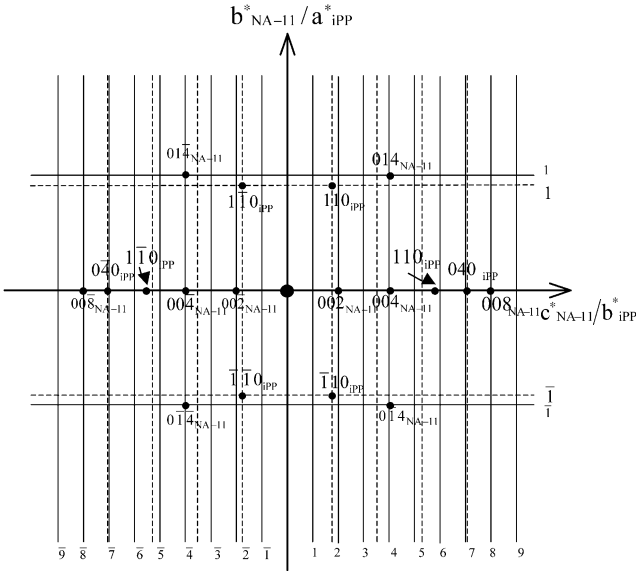

Fig. 7. Schematic representation of electron diffraction patterns of Figs. 3(b) and 5(b). The net patterns drawn with solid and dotted lines correspond to those of NA-11 and iPP, respectively.

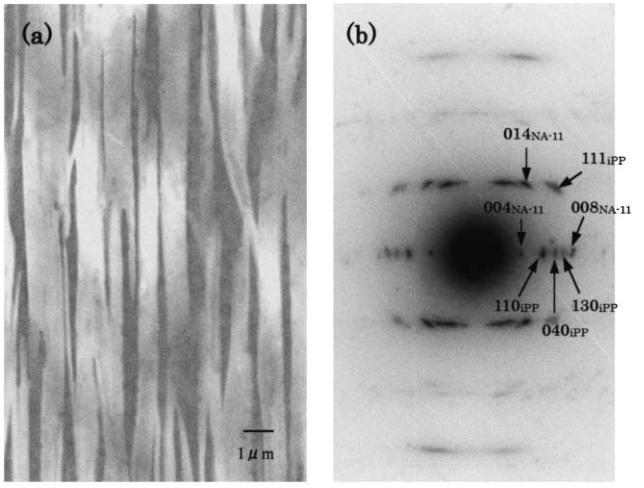

Fig. 8. Electron micrograph of the iPP film on which NA-11 crystals were grown from the solution in dimethylformamide at 140°C, and (b) the corresponding electron diffraction pattern. The molecular axis of iPP is vertical.

equator. From the indexing, it is definite that the net pattern of NA-11 crystals overlaps on the iPP fiber pattern with the *b*-axis of NA-11 parallel to the fiber axis of iPP, i.e. the *c*-axis. At higher crystallization temperatures, the oriented over-growth of NA-11 crystals occurs readily, and the lowest crystallization temperature where this orientation is achievable is around 120°C. Importantly, this orientational relationship is just corresponding to the second case described above. No other orientational relationship is identified. We discussed above that two modes of orientational relationship might occur when iPP is crystallized on NA-11 crystals. If iPP crystallizes directly on NA-1 crystals with the two different modes, it is also expected that in the reverse case where NA-11 is crystallized on iPP, NA-11 crystals would also grow exhibiting two orientations of crystallites with respect to the fixed *c*-axis of iPP, performing the above two orientational relationships. However, only the second type of orientational relationship mentioned above is identified. Taking these results into account, we conclude at least that the following epitaxial crystallization takes place preferentially; $[010]_{NA\text{-}11}//[001]_{iPP}$ and $(001)_{NA\text{-}11}//(010)_{iPP}$. In this epitaxial mode, the crystallographic relationship of the *a*-axis of NA-11//the *a*-axis of iPP results in. In Table 1, the crystallographic data of both crystals of NA-11 and α form of iPP are compared. The *c* cell dimension of iPP is very close to the *b* cell dimension of NA-11, and further the *a* cell dimension of NA-11 is about four times the *a* value of iPP cell. It is found that the lattice matching is able to be performed between two crystal lattices. In this orientation, the $(001)_{Na\text{-}11}$ is in contact with the $(010)_{iPP}$ plane.

We shall consider the above epitaxial relationship in the molecular level. The molecular model is shown in Fig. 9. From the results of structure analyses of NA-11 [4], it is shown that the pitch of iPP helix is comparable to the interval of tertial butyl groups arrayed in the direction parallel to the *b*-axis of NA-11 crystals. It is assumed that when iPP chains and NA-11 molecules are disposed side-by-side in such a way as the protrusion of iPP could be inlaid in the concave of NA-11 surface. From the ED patterns of Figs. 3–6, we set up two modes of orientational relationships, but eventually conclude that the second mode of epitaxial is preferential. Only from the lattice matching, the first mode of epitaxy is considered possible. However, it seems that such a definite molecular accommodation as in Fig. 9 would not be attained in this mode at the interface between two crystals in contact.

Figs. 4(a) and 6(a) show EMs of iPP after NA-11 crystals were removed. Concave traces are left after removal of NA-11. In Fig. 4(a), longitudinal concaves corresponding to the rod-like crystals of NA-11 are seen, and additionally, striations run perpendicular to them. The striations are corresponding to the iPP crystallites. In Fig. 6(a), oval-shaped concave forms with a rim like a cliff. This morphological feature explains that iPP crystallites mainly grow

Table 1
Lattice parameters of isotactic polypropylene (iPP) and NA-11

	Form	*a* (nm)	*b* (nm)	*c* (nm)	α (deg)	β (deg)	γ (deg)	System
IPP	α-form	0.665	2.096	0.65	90	99.2	90	Monoclinic
NA-11		2.6438	0.608	3.7172	90	93.65	90	Monoclinic

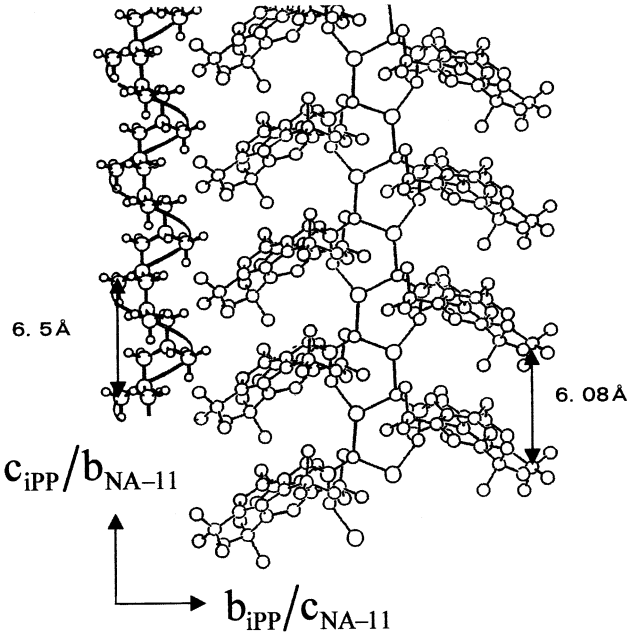

Fig. 9. Molecular fitting manner at the interface between iPP and NA-11 crystals.

perpendicularly to the lateral surface at the rim of NA-11 crystal, i.e. onto the (001) plane and not on the top surface. Fig. 10 details the fine texture of iPP formed laterally on the NA-11 crystals. In the morphology of Fig. 6(a), the detail of crystalline state of iPP is not revealed because iPP crystals grow thick at the rim of NA-11 crystals. Rod-like crystallites extend normal to the long axis of NA-11 in Fig. 10. This morphological feature may be basic in the growing process, but the molecular orientation in the single rods is unclear at the present time. It is concluded here that the epitaxial crystallization occurs with the axial relationship of $[001]_{iPP}//[010]_{NA-11}$. However, the first type of orientation appears to be a prevailing orientation in Figs. 3(b) and 5(b). It is well-known that iPP forms the cross-hatched texture through the homoepitaxy: iPP crystals grow by changing the molecular orientation by fitting the *a*-axis to the *c*-axis and vice-versa as the crystallites extend in the direction parallel to the *b*-axis [5–7]. On the basis of this homoepitaxy, occurrence of the first type of orientation can be explained as follows: iPP crystals first grow on the surface of NA-11 with the above epitaxial mode, i.e. their *c*-axis is parallel to the *b*-axis of NA-11 crystals. As iPP crystallites grow in the direction of the *b*-axis, their molecular orientation could be changed by adjusting the *a*-axis to the *c*-axis through the homoepitaxial mechanism [8]. This leads to the first type of molecular orientation. Thus, the orientational relationship is explained even if it is not the direct result from the epitaxial growth.

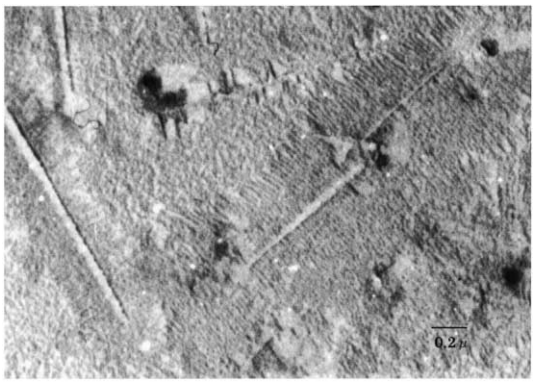

Fig. 10. Morphology of thin iPP crystallites crystallized on NA-11 crystals. NA-11 crystallites were removed with ethanol. Bright concaves are traces of NA-11 crystals left after washing with ethanol.

4. Concluding remarks

When epitaxial crystallization takes place, the rate of nucleation increases because the free energy barrier of nucleation is reduced. From this, we see that if the rate of crystallization is set to be the same, the crystallization should proceed at a higher temperature in case the epitaxial crystallization occurs. In the processing of iPP with NA-11 as nucleating agent, it crystallizes at a higher temperature than in the case of crystallization through the homogeneous nucleation process. Now that it is made clear that NA-11 crystals induce the epitaxial crystallization of iPP on them, it is generally concluded that effectiveness of nucleating agents is due to whether or not they cause the epitaxial crystallization.

Acknowledgements

This work is partly supported by a Grant-in-Aid for Scientific Research on Priority Area, ‘Mechanism of Polymer Crystallization’ (No.12127207), from the Ministry of Education, Culture, Sports, Science and Engineering, Japan.

References

[1] Haruna T, Tobita E. Soc Plastics Eng ANTEC’93, Detroit, MI.
[2] Petermann J, Gohil PRM. J Mater Sci 1979;14:2260.
[3] Natta G, Corradini P. Nuovo Cimento 1960;VX(X):40–51.
[4] Unpublished data.
[5] Lotz B, Wittmann JC. J Polym Sci Polym Phys Ed 1986;23:1541.
[6] Lotz B, Wittmann JC. J Polym Sci Polym Phys Ed 1986;23:1559.
[7] Masada I, Okihara T, Murakami S, Ohara M, Kawaguchi A, Katayama K. J Polym Sci Polym Phys Ed 1993;31:843–52.
[8] Yan S, Katzenberg F, Petermann J, Yang D, Shen Y, Straupe C, Wittmann JC, Lotz B. Polymer 2000;41:2613–25.